The value for K_{IC} is nearly independent of the grain size. This is also the case for sintered Al_2O_3 with MgO-doping, see for instance [12–14].

The fracture toughness is also independent on the CaO content. Ca, however, is a well-known segregant on grain boundaries in ceramic materials [3, 4, 15]. Jupp *et al.* [3] measured a drop in fracture toughness for intergranular fracture in commercial opaque alumina with increasing Ca content in the grain boundaries (as measured by Auger spectroscopy). In the case of transgranular fracture, as we have observed, one would expect no (if only a small) influence of the CaO-dope on K_{IC}. This is confirmed by our experiments.

References

1. L. A. SIMPSON and G. J. MERRETH, *J. Mater. Sci.* 8 (1974) 685.
2. G. K. BANSAL, in "Ceramic Microstructures '75", edited by R. M. Fulrath and J. A. Pask (Westview Press, Boulder, Colorado, 1970) p. 860.
3. R. S. JUPP, D. F. STEIN and D. W. SMITH, *J. Mater. Sci.* **15** (1980) 96.
4. A. W. FUNKENBUSCH and D. W. SMITH, *Metall. Trans.* **6A** (1975) 2259.
5. G. J. OUDEMANS, *Philips Technical Rev.* **29** (1968) 45.
6. *Idem, Proc. Brit. Ceram. Soc.* **12** (1969) 83.
7. R. J. KLEIN-WASSINK, *High Temp.–High Press.* **3** (1971) 411.
8. J. G. J. PEELEN, *Ceramurgia Int.* **5** (1979) 70.
9. G. WILLMAN and G. HEIMKE, *Prakt. Metall.* **15** (1978) 11.
10. E. E. UNDERWOOD, in "Quantitative Microscopy", edited by R. T. Dehoff and F. N. Rhines (McGraw-Hill, New York, 1968) p. 149.
11. W. F. BROWN and S. E. SRAWLEY, *ASTM-STP-410.*
12. J. D. B. VELDKAMP and N. HATTU, *Philips J. Res.* **34** (1979) 1.
13. P. L. PRATT, *Met. Sci.* **16** (1980) 363.
14. R. W. RICE, *Treat. Mater. Sci. Tech.* **11** (1977) 200.
15. M. PAULUS, *Mater. Sci. Res.* 3 (1966) S31.

Received 12 June
and accepted 18 July 1980

G. DE WITH
N. HATTU
Philips Research Laboratories,
Eindhoven,
The Netherlands

Strengthening of an austenitic stainless steel alloy by cryoforming

Cryoforming involves strengthening by transformation during plastic deformation at cryogenic temperatures. Since the process involves deformation at temperatures below ambient temperatures, it is most usefully applied to materials with M_s and M_d temperatures below room temperature. M_s is the temperature at which spontaneous allotropic transformation would occur and M_d is the highest temperature at which allotropic transformation can be induced by plastic deformation.

Several investigators [1–6] have studied the improvement of the mechanical properties produced in various materials by cryoforming. Prominent among the materials known to be favourably affected by cryoforming are the austenitic stainless steels. Deformation at cryogenic temperatures induces martensitic transformation in these materials, leading to improved strength. Foster Wheeler Corporation [7] and Arde Inc. [8] have successfully applied the process to the manufacture of stainless steel pressure vessels. A large proportion of previous investigations into the effects of cryoforming have involved evaluation of room-temperature properties. Since these materials also find application at cryogenic temperatures, in this study, the effects of cryoforming on the cryogenic mechanical properties of an austentic stainless steel alloy were investigated by testing the cryoformed material at a temperature of -196° C.

Qualitative and quantitative correlations have been attempted between the extent of martensitic transformation and the cryogenic yield strength of the cryoformed material and a mechanism of strengthening has been proposed. A low alloy austentic stainless steel was selected for this study since alloys of this grade have been observed to be most favourably affected by cryoforming. The composition and tensile properties of the alloy are shown in Tables I and II, respectively. Magnetic measurements, X-ray diffraction techniques and optical metallography were used to ascertain that

 0022–2461/81/030844–06$02.60/0

TABLE I Chemical composition (wt %) of the annealed material*

C	Mn	P	S	Si	Ni	Cr	Mo	Cu	Fe
0.07	1.89	0.028	0.018	0.51	8.60	19.03	0.31	0.25	Bal.

*Average of readings from 3 different specimens.

the as-received material was indeed all austenitic [9].

Cryoforming and testing were carried out on a universal tensile testing machine modified for cryogenic testing. A stainless steel dewar, fitted with pull rods and pin connectors to facilitate tensile loading, served as the cryostat (Fig. 1). Flat, pin-loaded, tensile specimens with 5.1 cm gauge sections were used. All pre-straining was carried out in tension at temperatures of -196° C and -73° C. Some specimens were also deformed at room temperature (25° C) in order to try to evaluate the advantages of cryoforming. Tensile testing was carried out only at -196° C. For cryostraining and testing at -196° C liquid nitrogen was used as the cryogenic medium. For deformation at -73° C, the cryostat was filled with isopropyl alcohol and liquid nitrogen was circulated through a copper coil placed in the dewar. The temperature of the alcohol was controlled by a solenoid valve regulated by a potentiometer and the temperature was monitored using a thermocouple. A stain rate of approximately 0.5 min^{-1} was used for both cryostraining and testing. Specimens were deformed to 50%, 75% and 90% of the ultimate strain, ϵ_u, respectively, at each of three temperatures, -196° C, -73° C and room temperature (25° C). They were subjected to natural aging treatments for up to 6 weeks. A minimum of 3 specimens were subjected to each set of thermomechanical treatments, at least two of which were later tested at -196° C. The remaining specimens were retained for metallographic studies. A few specimens were deformed to intermediate strain levels (62.5% ϵ_u, 85% ϵ_u) and tested at -196° C to provide a better correlation of deformation level with strength.

The volume fraction of martensite, $V_{\alpha'}$, produced by cryoforming was determined by precision density and magnetometric methods. For each set of cryoforming parameters, (level of deformation, temperature of deformation), the gauge section of one specimen was sectioned off and used for this part of the study. From X-ray diffraction studies, it was observed that all the thermomechanically processed samples were either a mixture of a martensite, α' and austenite, γ, or fully martensitic [9]. The density method, used to determine the volume fractions of the two phases is described in detail in [10]. The density, ρ, of the partially transformed material is given by:

$$\rho = \rho_\gamma V_\gamma + \rho_{\alpha'} V_{\alpha'}, \quad (1)$$

where ρ_γ and ρ_α are the densities of austenite and martensite, respectively, and V_γ and $V_{\alpha'}$ are the volume fractions of austenite and martensite, respectively. Since

$$V_{\alpha'} + V_\gamma = 1, \quad (2)$$

Equation 1 becomes

$$V_{\alpha'} = \frac{\rho_\gamma - \rho}{\rho_\gamma - \rho_{\alpha'}}. \quad (3)$$

TABLE II Mechanical properties of the annealed material

Temperature, T ($^\circ$ C)	Yield strength, S_y (MPa)	Tensile strength, S_u (MPa)	Ultimate strain, ϵ_u*	Area reduction, (%)
− 196	726	1549	0.33	34
− 196	786	1579	0.32	30
− 73	581	1104	0.36	42
− 73	636	1097	0.36	42
25	413	656	0.36	48
25	439	645	0.36	46

*ϵ_u is the true strain at maximum load.

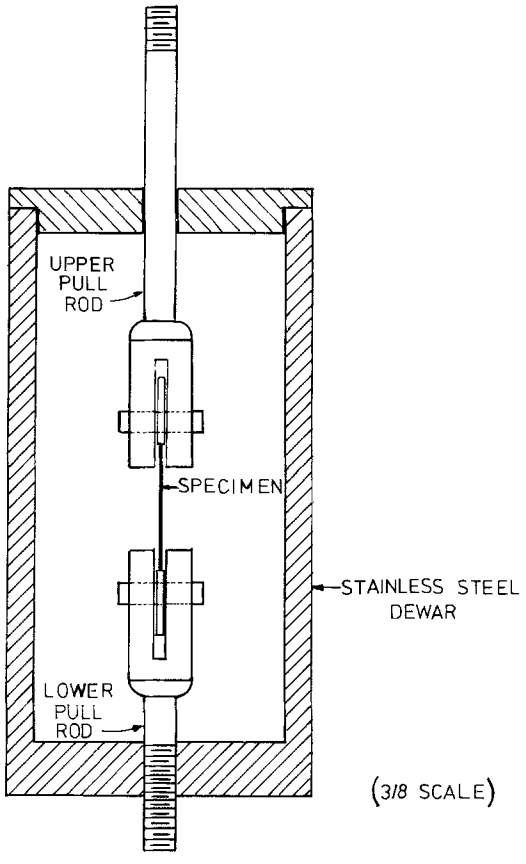

Figure 1 Section through cryostat showing the relative sizes of specimen and pull rods.

Error analysis on this method of determination of composition using density measurements showed that the technique is capable of determining the volume fraction percent of martensite present to within ± 5%. Within these limits any density change resulting from plastic deformation of the cryoformed material was found to be negligible, and no correction to this was therefore necessary.

The density of the pure austenite was determined to be 7.9584 gm cm^{-3}. A specimen deformed to 90% of the ultimate strain, ϵ_u, at − 196° C was found, by X-ray diffraction, to be completely martensitic in type [9]. This specimen was used to determine the density of pure martensite to be 9.8133 gm cm^{-3}. The accuracy of the latter density value is dependent on the accuracies of the X-ray and density methods. Since the strain-induced martensite transformation hardly ever goes to completion, it is suspected that the material identified as completely martensitic in type may have been only 95% so, reflecting an error of 5%. The magnetometric method was used to confirm the martensite volume fractions obtained by the density technique [9].

The load–elongation curves obtained from tensile tests on the as-received material showed plateau regions, characteristic of martensitic transformation, in specimens tested at − 196° C and − 73° C (Fig. 2) but not in those tested at room temperature. This was evidence that the M_d temperature of the alloy was higher than − 73° C but lower than room temperature. The load–elongation curve of the material tested at room temperature showed only a strain-hardening plastic region. On the other hand, those curves obtained by testing at the two cryogenic temperatures showed three different regions in the plastic range, as shown in Fig. 2. These regions have been identified as representing three distinct phenomena. The region a-b represents yielding and strain hardening of the parent austenite-phase. The almost horizontal region b-c represents rapid martensitic transformation under applied stress. The region c-d represents work hardening of both retained austenite and freshly-formed martensite, accompanied by further transformation of retained austenite to martensite. Similar results have been reported by other investigators [11–13].

The effects of processing parameters on mechanical properties were evaluated by testing at − 196° C. The yield strength at − 196° C and martensite content of specimens deformed at

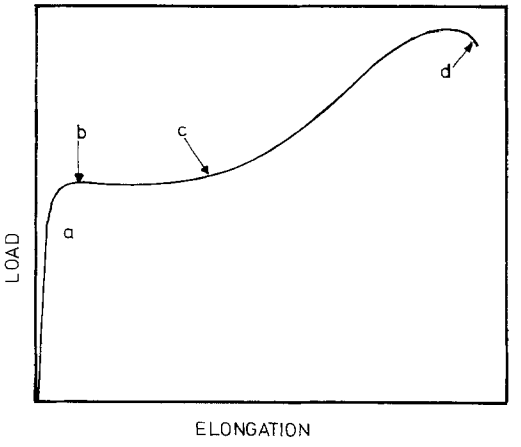

Figure 2 Schematic drawing of load elongation curve tor specimens deforming below M_d.

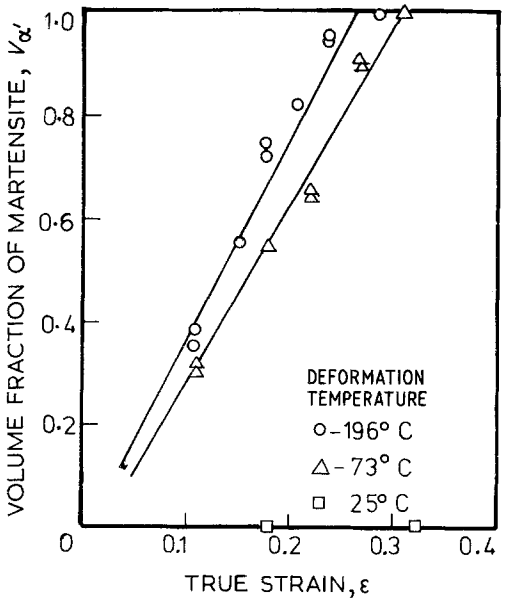

Figure 3 Effects of temperature and level of deformation on martensite content.

$-73°$ C and $-196°$ C increased with increasing deformation (Figs 3 and 4). A linear relationship

$$V_{\alpha'} = A\epsilon + B, \quad (4)$$

where A and B are constants, fits the data. For a deformation temperature of $-196°$ C, $B = -0.02$ and $A = 3.85$; for a deformation temperature of $-73°$ C $B = -0.07$ and $A = 3.48$. Angel [11] has reported a sigmoidal relation between $V_{\alpha'}$ and ϵ with the departures from linearity occurring at very high and very low strains. It is entirely possible that the data obtained in the present study represent the linear portions of a sigmoidal relationship. The constant A in Equation 4 is the same as the transformation coefficient defined by Gerberich *et al.* [14]. As the deformation temperature decreased below M_d the stability of the austenite decreased and the rate of transformation with strain increased. The stacking fault energy (SFE) of the austenite is directly related to stability through its role in initiating the γ–α' transformation. Since the SFE of Fe–N–Cr alloys increases linearly with increasing temperature, decreasing the temperature reduces the austenite stability [13]. It should be noted, once again, that specimens identified to be of 100% martensitic-type (Fig. 3) may be only 95% as a result of the accuracy of the density method.

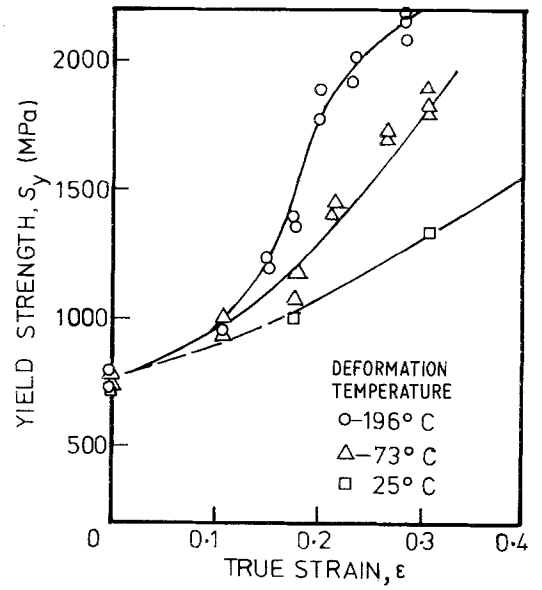

Figure 4 Effects of temperature and level of deformation on yield strength.

A summary of the mechanical properties of the cryoformed material is presented in Table II. Cryogenic yield strengths of over 1800 MPa with ductility in excess of 10% area reduction have been produced by thermomechanical treatment.

Since further martensitic transformation occurred during tensile testing, only the yield strength could be directly related to the structure of the thermomechanically-treated alloy. The work-hardening rate increased with progressive transformation, making it meaningless to relate the tensile strength to the microstructure of the as-processed material. The martensite transformation has also been observed to affect ductility [9, 11–13]. As with the tensile strength, it would therefore be meaningless to correlate ductility and the martensite content of the cryoformed material since further transformation occurred during testing. In the absence of a stress-induced martensitic transformation, as was the case in this study, the yield strength is directly related to the structure of the thermomechanically-treated alloy.

The following relationships were established between the yield strength at $-196°$ C, S_y, and the volume fraction of martensite, $V_{\alpha'}$, (see Fig. 5):

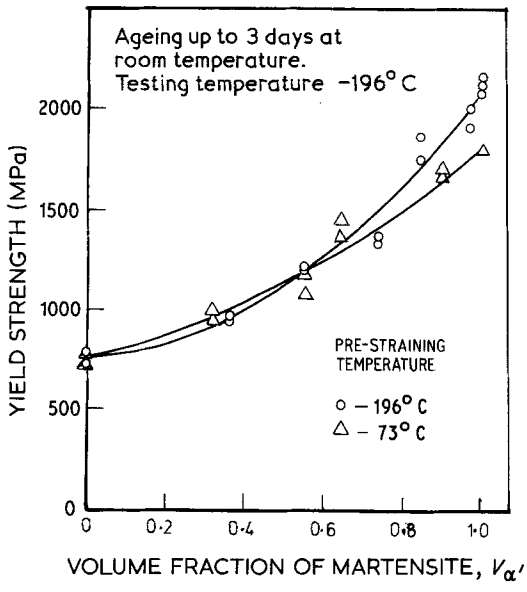

Figure 5 Correlation between yield strength and volume fraction of martensite.

(a) for specimens prestrained at − 196° C,

$$S_y = 756 + 1326 V_{\alpha'}^{1{\cdot}88}; \quad (5)$$

(b) for specimens pre-strained at − 73° C,

$$S_y = 756 + 1002 V_{\alpha'}^{1{\cdot}32}. \quad (6)$$

The values S_y for $V_{\alpha'} = 0$ in both equations represents the yield strength of the annealed material at − 196° C.

The improved cryogenic yield strength of the cryoformed and naturally-aged material was due to the formation of strain-induced martensite and work hardening of both the freshly-formed martensite and retained austenite. At low pre-strain levels, strengthening was predominantly due to strain-induced martensite. At higher pre-strain levels, strain hardening of martensite and austenite contributed significantly to the yield strength.

Strengthening mechanisms so far proposed for cryoformed austenitic stainless steels have neglected the contribution of strain hardening [15, 16]. The load–elongation curve of the annealed material tested below M_d temperature showed a strong effect of strain hardening at high strains. It is not surprising that strain hardening should contribute to the cryogenic mechanical properties of highly pre-strained specimens.

Acknowledgements

The author wishes to thank Professors Tom Scott and Alexander Henkin of Iowa State University for their guidance during the course of this study. Special thanks are also due to Messrs B. Kanetsi and B. C. Paul of the University of Zambia for their contributions towards the production of this paper.

References

1. W. O. BINDER, *Met. Prog.* 58 (1950) 201.
2. V. N. KRIVOBOK and A. M. TALBOT, *Proc. ASTM* 50 (1950) 895.
3. D. W. McDOWELL and J. R. MIHALISIN, *Mater. Eng. Design* 53 (1961) 10.
4. D. T. LLEWELLYN and J. D. MURRAY, Iron and Steel Institute Special Report No. 86 (1964) 197.
5. H. C. FIELDER, B. C. AVERBACH and M. COHEN, *Trans. ASM* 47 (1955) 267.
6. C. R. MAYNE, ASTM Special Technical Paper No. 287 (1960) p. 150.
7. L. KUNSAGI, M. SVEND and W. R. APBLETT, Jr, "Method for the Explosive Section Forming of Pressure Vessels", Foster Wheeler Corp., New York, U.S. Patent No. 3,344,509, October, 1967.
8. "The Ardeform Process" Report No. P-30715C,

TABLE III Summary of mechanical properties at − 196° C

Deformation temperature (° C)	Level of deformation (% of ϵ_u)*	Yield strength (MPa)	Tensile strength (MPa)	Area reduction (%)
− 196	90	2076	2081	5
− 196	90	1860	1925	15
− 196	50	1255	1843	20
− 73	90	1850	1920	20
− 73	50	1255	1700	26
25	90	1306	1782	28
25	50	1062	1715	23

*ϵ_u is the true strain at maximum load.

Arde–Portland Inc., Paramus, New Jersey, U.S. Patent No. 3,197,851, January 1964.
9. J. OPOKU, Ph.D. Dissertation, Iowa State University, Ames, Iowa, 1977.
10. F. X. KAYSER, A. LITWINCHUK and G. L. STOWE, *Met. Trans.* **6A** (1975) 55.
11. T. ANGEL, *J. Iron and Steel Inst.* 177 (1954) 165.
12. J. P. BRESSANELLI and A. MOSKOWITZ, *Trans ASM* 59 (1966) 223.
13. D. BHANDARKAR, V. F. ZACKAY and E. R. PARKER, *Met. Trans.* 5 (1972) 2619.
14. W. W. GERBERICH, G. THOMAS, E. R. PARKER and V. F. ZACKAY, Proceedings of the Second International Conference on the Strength of Metals and Alloys, Asilomar, California, August, 1970 p. 894.
15. P. L. MANGONON and G. THOMAS, *Met. Trans.* 1 (1970) 1587.
16. N. V. NOVIKOV and N. I. GORODYSKII, *Met. Sci. Heat Treatment* 17(2) (1975) 164.

Received 14 May
and accepted 23 July 1980

JUSTIN OPOKU
School of Engineering,
University of Zambia,
Lusaka
Zambia

X-ray determination of lattice parameters and thermal expansion of potassium bromate

The lattice parameters of potassium bromate ($KBrO_3$) have been determined by different investigators (Swanson *et al.* [1], Mery [2] and Wyckoff [3]) but only at room temperature. No data are available on the temperature variation of the lattice parameters either at low or high temperatures. Also thermal expansion of $KBrO_3$ has not previously been measured. Hence it was decided to investigate the properties of $KBrO_3$ with the object of determining the lattice parameters and thermal expansion as a function of temperature between 302 and 512 K.

Powder samples of $KBrO_3$ with a specified purity of 99.99% were obtained from Riedel Dettan Ag Seelze, Hannover, Germany. To obtain uniform particle size these powder samples were filtered through a 44 μm sieve.

A symmetrically focusing back-reflection camera of 15 cm diameter was used for obtaining powder photographs at elevated temperatures with filtered CuKα radiation. The specimen holder and heater were of such a design that the specimen could be heated to and maintained at any desired temperature. The temperature of the specimen could be measured to an accuracy of ± 0.8 K with the help of Pt–13% Rh thermocouple and a commercial temperature controller. The powder photographs were obtained at thirteen intervals between 302 and 512 K.

The X-ray powder photograph showed ten intense lines in the angular range from 72° to 82° i.e. $(6\,1\,2)_{\alpha_1\alpha_2}$, $(6\,1\,1)_{\alpha_1\alpha_2}$, $(4\,2\,6)_{\alpha_1\alpha_2}$, $(4\,0\,8)_{\alpha_1\alpha_2}$ and $(3\,3\,6)_{\alpha_1\alpha_2}$. The $KBrO_3$ has a rhombohedral structure. In evaluating the lattice parameters of $KBrO_3$ using Bragg reflections, it was assumed that rhombohedral structure is a special case of hexagonal structure. The a and c lattice parameters were evaluated at different temperatures using Cohen's analytical method [4]. Independent measurements and calculations were made on each film and the average values obtained from these are given in Table I.

Wykoff [3] and Mery [2] quoted the room temperature values of the lattice parameters but without any reference points or experimental

TABLE I Lattice parameters of potassium bromate at various temperatures

Temperature (K)	a_T (Å) (± 0.0003)	c_T (Å) (± 0.0009)
302	6.0170	8.1935
324	6.0232	8.1978
341	6.0279	8.2015
358	6.0341	8.2056
379	6.0390	8.2089
394	6.0436	8.2148
400	6.0456	8.2167
410	6.0503	8.2255
425	6.0554	8.2301
446	6.0611	8.2365
462	6.0661	8.2448
486	6.0760	8.2601
512	6.0841	8.2747

0022–2461/81/030849–03$02.30/0